Microstructure and mechanical properties of ZrB2-SiC composites fabricated by the centrifugal gel casting

Jingmao Chen
Harbin Institute of Technology
Dongyang Zhang (zhangdyhit88@163.com)
Harbin Institute of Technology
Ping Hu
Harbin Institute of Technology
Shun Dong
Harbin Institute of Technology
Xinghong Zhang
Harbin Institute of Technology

Research Article

Keywords: ZrB2-SiC; Centrifugal gel casting; Pressureless sintering; Mechanical properties

Posted Date: April 8th, 2020

DOI: https://doi.org/10.21203/rs.3.rs-21450/v1

Abstract

The high-performance and reliable ZrB_2-SiC composites were fabricated by centrifugal gel casting and pressureless sintering. A well-dispersed ZrB_2-SiC suspensions with up to 48 vol.% solid loading was achieved by adding 0.6 wt.% PAA dispersant and adjusting pH value to 11. The crack-free green ZrB_2-SiC ceramic bodies with homogenous microstructure were prepared successfully by centrifugal gel casting with a relatively low monomer content of 3.5wt.% and centrifugal speed of 9000 r/min. After pressureless sintering at 2000 °C for 1 h, ZrB_2-SiC composites with a relative density of 94.8%, a flexural strength of 394 ± 14 MPa and fracture toughness of 4.03 ± 0.10 MPa·$m^{1/2}$ were achieved. This approach provided a promising colloidal processing to fabricate ceramic composites with reliable properties.

1. Introduction

Zirconium diboride (ZrB_2) as a vital member of ultra-high temperature ceramics (UHTCs) classes is a subject of interest due to its high melting point, high hardness, superior strength, good electric and thermal conductivities, resistance to corrosion, as well as superb antioxidant ablation performance[1–4]. All these features make ZrB_2 and ZrB_2-based ceramics attractive for ultra-high temperature applications, such as sharp nosecones, leading edges and propulsion components, thermal protection system for hypersonic aerospace vehicles and advanced reusable atmospheric reentry vehicles [5–8].

As with other nonoxide ceramics, ZrB_2 would be easy to be oxidized when exposed to air under an elevated temperature, the addition of second phase SiC particles would enhance the oxidation resistance by decreasing oxidation rate of ZrB_2 [2, 9, 10]. Generally, ZrB_2-SiC ceramics are usually fabricated by hot pressing or spark plasma sintering [11], which limit the fabrication of samples with relatively simple geometrical and moderate size, and requires costly and time-consuming electrical machining to obtain complex-shaped components. Recently, a great number of colloidal processing have been used to prepare near-net shaped components, such as tape casting [12], slip casting [13], centrifugal casting [14] and gel casting [15]. Among the colloidal processing, the most suitable process is gel casting that enables the materials to achieve higher microstructural homogeneity and high strength in green and sintered parts with complex shapes. Gel casting is a generic method based on a combination of traditional ceramics forming and polymer chemistry, including the homogeneous dispersion of ceramic powders into dissolved colloidal solutions and then casting into a sealed mould with in situ polymerization to form a macromolecular gel network to hold the ceramic particles together [16, 17]. However, the wet gelcasted green bodies were prone to shrink or crack owing to the non-uniform contraction in the process of removing the moisture [18]. He et al. [19] pointed out that a high solid loading in the suspensions could reduce shrinkage during drying and sintering processes. However, it must be noted that when the slurry viscosity increased as a consequence of the increase in the solid loading, the problem with air bubbles trapped in the suspensions become more critical [20]. Vacuum deairing would not work as efficiently as in the case of low viscosity slurries and it was essential to combine the mechanical stirring process with vacuum deairing to minimize the air bubbles [21].

Centrifugal casting process is one of the colloidal processings that has been used for many years of the fabrication of the ceramics [22]. A well-dispersed suspension was poured into a mould and then particles packing and casting was motivated by the centrifugal forces. The centrifugal field on the slurries could act as a purifying factor to eliminate air bubbled trapped in the suspensions and disrupt the larger heavy inclusions. Centrifugal casting with a high centrifugal acceleration was an effective way to eliminate significant mass segregation of particles for processing highly concentrated and multicomponent slurries. However, the number of the heterogeneities among particles was increased using centrifugal casting process, resulting in slightly detracting from the packing density and final properties of the ceramics [23]. In addition, the centrifugal accelerations used in centrifugal casting process to fabricate advanced ceramic materials were usually in the order of 2000–5000 g, which was reasonable to use higher spinning speeds instead of longer radius of centrifugation to achieve the specified centrifugal accelerations due to the equation of $\alpha = \omega r^2$. Besides, the time required for the centrifugal processing of submicrometer-sized concentrated slurries was as long as 1–2 hours [24], which was too long to keep the slurry under such severe centrifugation condition due to high energy consumption and high degree of machinery depreciation.

In this paper, we present a novel process called “centrifugal gel casting” (CGC), which combined the advantages of centrifugal casting and gel casting processes, enhancing particle packing and eliminating bubbles trapped in the green body via high centrifugal forces and in situ polymerization of the three-dimensional gel networks to cover particles. In the combined process, neither high centrifugal accelerations are required nor a long time for cast formation. The dispersion behaviour and rheology properties of ZrB_2-SiC suspensions were studied in detail, and the centrifugal parameters on the microstructure and relative density distribution of green bodies were analysed. In addition, the microstructure and mechanical properties of pressureless sintered parts were also characterized.

2. Experiments

2.1 Raw materials

Commercial powders were used for the materials preparation: ZrB_2 (Beijing HWRK Chem Co. Ltd., China) with an average particle size of 2 μm and SiC (Weifang Kaihua SiC Micro-powder Co. Ltd, Weifang, China) with an average particle size of 0.5 μm were used as raw materials. B_4C powders (Aladdin Reagent Co. Ltd, Shanghai, China) with an average particle size of 1 μm and phenolic resin (Shengquan Hi-tech Material Co. Ltd, Yinkou, China) with remaining 55% carbon were used as sintering additives. To obtain aqueous homogeneous gel solutions, deionized water was chosen as solvent, and acrylamide (CH_3CONH_2, AM, supplied by Aladdin Reagent Co. Ltd, Shanghai, China) and N,N’-methylenebisacrylamide ($(C_2H_3CONH)_2CH_2$, MBAM, supplied by Aladdin Reagent Co. Ltd, Shanghai, China) were used as monomer and cross-linker respectively. In addition, ammonium persulfate ($(NH_4)_2S_2O_8$, APS, supplied by Aladdin Reagent Co. Ltd, Shanghai, China) was applied as initiator. Polyacrylic acid (PAA, Mw = 3000, supplied by Aladdin Reagent Co. Ltd, Shanghai, China) was added as

dispersant to obtain well-dispersed ZrB_2-SiC suspensions. Strong acid (HCl) and ammonia (NH_4OH) (supplied by Aladdin Reagent Co. Ltd, Shanghai, China) were used as pH adjusting regent. All of these analytical reagents were chemically pure.

2.2 Fabrication of composite

Figure 1 illustrated the flow chart of the centrifugal gel casting process. Firstly, a premix solution of colloidal additives was prepared in deionized water with 2-5wt.% (based on demonized water) AM monomer, and the ratio of cross-linker to monomer was 1:10. Subsequently, the ZrB_2-20 vol% SiC-4 vol% B_4C-2 vol% C mixed powders with different content (0.2-1.0 wt.%, based on mixed powders) of PAA dispersant were added in the mixed solutions. The solid loading of the slurries varied from 30 vol.% to 50 vol.% and then the pH of the slurries was adjusted by HCl and NH_4OH. In order to break down agglomerates, the slurries were ball-milled using ZrO_2 milling balls at a rotary speed of 250 rmp for 10 hours. For centrifugal gel casting, the APS initiator was injected by vigorous mixing and was poured into a PTFE mould for 5–20 min at centrifugal speed of 8000–9500 r/min in a centrifugal machine (TD-24K, Hunan Xiangyi Laboratory Instrument Development Co. Ltd., Hunan, China). After centrifugation, the mould containing ceramic green bodies was placed at 70 °C in water bath for 45 min for the gelation process completely. After drying freely in constant humidity (98%) and temperature (25 °C) for 30 h, the crack-free green bodies was achieved successfully. The binder burnout process of the centrifugal gel-casted samples was carried out in 800 °C for 2 h by a controlled heating rate of 1 °C/min for eliminating organic additives completely. Finally, the samples were pressureless sintered at 2000 °C for 1 h in an argon atmosphere. Both binder burnout and pressureless sintering processes were accomplished in a high temperature graphite resistant furnace (ZRY-80, Jinzhou Hangxing Vacuum Equipment Co. Ltd., Jinzhou, China).

2.3 Characterization

The zeta potentials of ZrB_2, SiC and ZrB_2-SiC suspensions (0.01 vol.% solid loading) with and without dispersant were measured by the Zeta potential analyzer (Malvern Zetasizer Nano, Malvern Instruments Ltd, UK), and the viscosities of ZrB_2-SiC slurries were investigated using a viscometer (DV-II + Pro, Brookfield Ltd, USA). The densities of the green bodies and the sintered parts were measured by the Archimedes method with deionized water as immersion medium. The microstructures of the green bodies and sintered parts were characterized by the scanning electron microscopy (SEM, FEI Sirion, Holland) with energy-dispersive spectroscopy (EDS). The X-ray diffraction (XRD) (Empyrean, PANalytical B.V., Netherlands) pattern of the sintered ceramics was measured with a Rigaku diffractometer using Cu-Kα radiation (α = 0.15418 nm). The flexural strength(σ) was measured by three-point bending tests (Model 5569, Instron, USA) on 3 × 4 × 36 mm^3 (thickness × width × length) test bars with a span of 30 mm and a cross-head speed of 0.5 $mm \cdot min^{-1}$ at room temperature, the fracture toughness (K_{IC}) was evaluated by single-edge notched bend (SENB) on 2 × 4 × 22 mm^3 (width × height × length), with a notched depth and width of 2 and 0.2 mm, respectively, using a span of 16 mm and cross-head speed of 0.05 $mm \cdot min^{-1}$.

3. Results And Discussion

3.1 The rheology properties of ZrB_2-SiC suspensions

The relationship between Zeta potentials of single ZrB_2 and single SiC slurries as well as ZrB_2-SiC suspensions with and without 0.5 wt.% PAA dispersion and pH value was presented in Fig. 2. According to the measurements, the isoelectric point (IEP, the pH value which the net charge on the particle surface was zero) for ZrB_2 and SiC slurries were 6.5 and 4.2, respectively. When PAA dispersant added, the value of IEP were from 6.5 to 6.2 for ZrB_2 suspension and from 4.2 to 3.8 and SiC suspension, respectively. Moreover, it was worth noted that the absolute Zeta potentials values of both ZrB_2 and SiC suspensions with PAA dispersion approached to the highest at pH 11 due to the dominated repulsive forces, indicating the well-dispersed suspensions with good fluidity were achieved. Furthermore, the absolute zeta potential value of ZrB_2-SiC suspensions also achieved to the highest level at pH 11 with PAA dispersant, which was attributed to the improvement of the electrophoresis mobility by dominant tails and loops configurations of PAA dispersant.

The high solid loading and low viscosity suspensions were the prerequisites for the preparation of high-performance ZrB_2-SiC ceramics by centrifugal gel casting process. The effect of PAA dispersant concentration on the viscosity of ZrB_2-SiC suspensions with 30 vol.% solid loading at pH 11 was presented in Fig. 3. It was worth noted that the suspensions with different PAA concentration all showed a “shear thinning” effect with viscosity decreasing as shear rate increasing. When PAA concentration approached to 0.6 wt.%, the ZrB_2-SiC suspension had a minimum viscosity of 0.57 Pa·S at 60 S^{-1}, indicating that electrostatic repulsion among the particles was greatly increased due to enhanced adsorption of PAA dispersant on the surface of the particles.

Neither high solid loading nor low solid loading has an adverse effect on the properties of the green bodies fabricated by the centrifugal gel casting procedure. Figure 4 presented the relationship between solid loading and viscosity of ZrB_2-SiC suspension (0.6 wt.% PAA dispersant at pH 11). It was worth noted that the viscosity of the suspensions under different solid loading showed a decreasing tendency as shear rate increasing, namely, “shear thinning” effect, which was attribute to the increased hydrodynamic interactions among ceramic particles [25]. The larger aggregates in the ceramic slurries were dissolved due to the shear force and the slurry tended to flow in the direction of rotation, so the ceramic slurries exhibited a shear thinning effect under the combined mechanism. Considering high solid loading and low viscosity were desirable for the following centrifugal gel casting processes. When the solid loading of the slurries was increased to 50 vol.%, the steric repulsion was inhibited due to the decreased particle spacing, resulting in a sharp increase in the viscosity of the slurries, which was not conducive for the centrifugal gel casting. Therefore, the high concentrated ZrB_2-SiC suspension up to 48 vol.% with low viscosity (1.50 Pa·S at 60 S^{-1}) was suitable for centrifugal gel casting process in our experiments.

3.2 The centrifugal gel casting process of ZrB_2-SiC ceramics

3.2.1 Effect of the monomer content on the properties of the ZrB_2-SiC ceramics

The influence of the monomer content on the microstructure of centrifugal gel-casted ZrB_2-SiC green bodies was presented in Fig. 5. When the monomer content was 2 wt.%, it was difficult to form three-dimensional networks to cover the ceramic particles, resulting in the localized particles agglomeration. When the monomer content increased to 3 wt.%, the primary free radical reactivity was too weak to produce the sufficient free radicals, resulting in decreasing the cross-linking solidification reaction to form a complete and uniform three-dimensional network structure, leaving more holes in the green ceramic bodies and ultimately affecting the properties of the ZrB_2-SiC green parts. While the three-dimensional gel networks could completely cover the ceramic powder and the holes or cracks of green bodies could be eliminated to enhance the mechanical properties of the green bodies as monomer content increased to 3.5 wt.% or above. However, it was worth noted that the organic gel networks were prone to aggregate together, which had adverse effects on the properties of sintered ZrB_2-SiC ceramics by producing more holes or cracks during the burnout processing when monomer content was increased up to 5 wt.%. Therefore, 3.5 wt.% monomer content was available to prepare ZrB_2-SiC green bodies with high particle packing and uniform distribution of particles owing to the in-situ three-dimensional and homogenous gel networks.

3.2.2 Effect of the centrifugal parameter on the relative green density of the ZrB_2-SiC ceramics

In order to investigate the influence of the centrifugal parameter (centrifugal speed and centrifugal time) on the elimination of air bubbles, the relationship between the relative green density of different parts (bottom, middle and top) and centrifugal parameter was presented in Fig. 6. When the centrifugal speed was low to 8000 r/min, the small average size of SiC particles was difficult to fill into the gap between and particles to particles of ZrB_2, resulting in the existence of large pores in the green ceramic bodies. When the centrifugal speed increased to 8500 r/min or above, the relative green densities were largely improved owing to the increased settle rate of ceramic particles. Notably, the relative green density gradient was the smallest and the relative green density could approach up to 60.6%, at which the bubbles and larger inclusions were eliminated by high centrifugal speed. The relative green density kept steady, but the relative density gradient increased when the centrifugal speed increased to 9500 r/min (Fig. 6a).

When the centrifugal time was less than 5 min, the settle distance of the particles in the ceramic suspensions was limited and the elimination of the bubbles was blocked, resulting in low relative green

density and enlarging relative density gradient from the bottom to the top of the green parts (Fig. 6b). However, the settle rate of the particles in the ceramic slurries was accelerated to improve the particles stacking via eliminating bubbles and filling the gap within ceramic particles when the centrifugal time extended to 10 min. When the centrifugal time extended to 15 min or more, the effect of the difference in deposition rate between ZrB_2 and SiC particles was dominant, resulting in enlarging the gradient of the relative green density from the bottom to the top, in which the phase separation could not be ignored. Therefore, the centrifugal parameters with centrifugal speed of 9000r/min and centrifugal time of 10 min were available to prepare the ZrB_2-SiC green bodies with high particle packing and homogenous distribution of the particles.

3.3 The drying and debinding process of ZrB_2-SiC ceramics

3.3.1 The drying process

In order to achieve crack-free ZrB_2-SiC green bodies, the centrifugal gel-casted ceramics were performed at constant temperature and humidity to avoid the occurrence of micro-cracks during drying process. Figure 7 showed the variation curve between mass loss and drying time of the centrifugal gel-casted green bodies. The drying curves showed a rapidly decrease in mass loss of green bodies in stage 1, which was attributed to the rapidly evaporation of the moisture on the surface of the green bodies. Then the drying force of capillary action was dominant to provide the diffusion route for the water evaporation from the inside to the outside after 22 drying hours, during which the drying rate was low and the mass loss kept constant to 4.95 wt.%. In order to avoiding crack occurred during the following debinding process, the drying time was extended to 48 h for the complete evaporation of the chemical bound water.

3.3.2 The debinding process

The organic additives incorporated into the ZrB_2-SiC green bodies should be removed before sintering, the TG-DSC experiment of the green bodies was conducted to obtain the optimum debinding parameters, as showed in Fig. 8. The removal of the chemical bound water caused a significant endothermic peak at 82.25 ºC, and the organic additives were burn out at 368.85 ºC accompanied by an obvious endothermic peak, resulting in a sharp weight loss rate of the green bodies. The endothermic peak at 496.84 ºC was mainly resulting from the degradation of residual carbon from organic additives. The residual water could be fully vaporized and the organic additives could be complete burnout as no mass loss when burnout temperature increased up to 600 ºC, leaving about 4.2 wt.% weight loss in the total debinding process. Therefore, the green bodies was heated up to 800 ºC at a heating rate of 1 ºC/min and kept 2 h for full debinding of the residual water and organic additives.

3.4 The microstructures and mechanical properties of sintered ZrB_2-SiC ceramics

The ZrB_2-SiC green bodies with optimum centrifugal gel-casting process (3.5wt.% monomer content, 9000r/min centrifugal spend with 10 min) was successfully achieved after drying and debinding processes, then the pressureless sintering with 2000 ºC for 1 h was conducted to obtain the ZrB_2-20 vol% SiC-4 vol% B_4C-2 vol% C ceramics. In order to analysis whether the phase segregation occurred in the centrifugal gel casting process, the XRD patterns of sintered ceramics from the bottom to the top regions were detected, as showed in Fig. 9. It was worth noted that the ZrB_2 and SiC main phase were detected in all regions and the diffraction peak intensity and width of ZrB_2 or SiC phase was consistent in each region from the bottom to the top, verifying no phase separation in each region of sintered ZrB_2-SiC ceramics.

Moreover, the density, flexural strength and fracture toughness were 94.8%, 394 ± 14 MPa and 4.03 ± 0.10 $MPa{\cdot}m^{1/2}$, respectively. And the microstructures of the polished surface of sintered ZrB_2-SiC ceramics were also analysed, as showed in Fig. 10. It was obvious that the dark phases of SiC particle were dispersed in gray phase of ZrB_2 matrix uniformly and no obvious agglomeration was detected. Moreover, the examination of the microstructures revealed an average grain size of about 4 μm for ZrB_2 grains and about 1 μm for SiC grains. In addition, it was believe that the centrifugal gel-casting process could be a promising method to fabricate multiphase ceramics with homogenous microstructure and excellent mechanical properties.

4. Conclusions

A novel method was called centrifugal gel casting of improving green bodies microstructure and reliability of the final product by combining gelcasting and centrifugal casting processes. The ZrB_2-SiC ceramics with homogenous phase distribution was successfully fabricated by the centrifugal gel casting process and pressureless sintering. A well-dispersed ZrB_2-SiC suspension with solid loading up to 48 vol.% and low viscosity was achieved by adding 0.6 wt.% PAA dispersant and adjusting pH value to 11. Then the ZrB_2-SiC green ceramics with high particle packing and homogenous phase distribution were fabricated with centrifugal speed of 9000r/min for 10 min. The drying was conducted in a constant temperature and humidity for 48 h to evaporate the chemical bound water of the green bodies, and the debinding was conducted at 800 ºC for 2 h to remove the residual water and organic additives completely. Finally, sintered ZrB_2-SiC ceramics was obtained after pressureless sintering at 2000 ºC for 1 h, and the density, flexural strength ad fracture toughness were 94.8%, 394 ± 14 MPa and 4.03 ± 0.10 $MPa{\cdot}m^{1/2}$, respectively. This work combined the gel casting and centrifugal casting together to overcome the existing limitations and disadvantage for the fabrication of multiphase ceramics with high particle packing and on phase separation.

Declarations

This work was supported by the National Natural Science Foundation of China (No.51872059, 51772061, and 51902067), the National Fund for Distinguished Young Scholars (51525201), the China Postdoctoral

Science Foundation (2019M651282).

References

1. MM Opeka, IG Talmy, EJ Wuchina, et al. Mechanical, thermal, and oxidation properties of refractory hafnium and zirconium compounds, J. Eur. Ceram. Soc. 19 (1999) 2405-2414.
2. WG Fahrenholtz, GE Hilmas, IG Talmy, et al. Refractory diborides of zirconium and hafnium, J. Am. Ceram. Soc. 90 (2007) 1347-1364.
3. F S Moghanlou, M Vajdi, J Sha, et al. A numerical approach to the heat transfer in monolithic and SiC reinforced HfB_2, ZrB_2 and TiB_2 ceramic cutting tools, Ceram. Int. 45 (2019) 15892-15897.
4. R Zhang, X Cheng, D Fang, et al. Ultra-high-temperature tensile properties and fracture behavior of ZrB_2-based ceramics in air above 1500°C. Mater. Des. 52 (2013) 17-22.
5. E P Simonenko, D V Sevast'yanov, N P Simonenko, et al. Promising ultra-high-temperature ceramic materials for aerospace applications, Russ. J. Inorg. Chem, 58 (2013) 1669-1693.
6. W G Fahrenholtz, G E Hilmas. Ultra-high temperature ceramics: Materials for extreme environments. Scrip. Mater, 129 (2017) 94-99.
7. X Zhang, P Hu, J Han, et al. Ablation behavior of ZrB_2-SiC ultra high temperature ceramics under simulated atmospheric re-entry conditions. Compos. Sci. Technol. 68 (2008) 1718-1726.
8. N P Padture. Advanced structural ceramics in aerospace propulsion. Nat. Mater. 15 (2016) 804-809.
9. F Li, C Tan, J Liu, et al. Low temperature synthesis of ZrB_2-SiC powders by molten salt magnesiothermic reduction and their oxidation resistance, Ceram. Int. 45 (2019) 9611-9617.
10. D Zhang, P Hu, S Dong, et al. Oxidation behavior and ablation mechanism of Cf/ZrB2-SiC composite fabricated by vibration-assisted slurry impregnation combined with low-temperature hot pressing, Corros. Sci. 161 (2019) 108181.
11. R Stadelmann, M Lugovy, N Orlovskaya, et al. Mechanical properties and residual stresses in ZrB_2-SiC spark plasma sintered ceramic composites. J. Eur. Ceram. Soc. 36 (2016) 1527-1537.
12. Z Lü, D Jiang, J Zhang, et al. Aqueous tape casting of zirconium diboride, Am. Ceram. Soc. 92 (2009) 2212-2217.
13. S Leo, C Tallon, G V Franks. Aqueous and nonaqueous colloidal processing of difficult-to-densify ceramics: suspension rheology and particle packing, Am. Ceram. Soc. 97 (2014) 3807-3817.
14. P Rao, M Iwasa, T Tanaka, et al. Centrifugal casting of Al_2O_3-15wt.%ZrO_2 ceramic composites, Ceram. Int. 2003, 29 (2003) 209-212.
15. R He, X Zhang, P Hu, et al. Aqueous gelcasting of ZrB_2-SiC ultra high temperature ceramics, Ceram. Int. 38 (2012) 5411-5418.
16. OO Omatete, MA Janney, SD Nunn. Gelcasting: from laboratory development toward industrial production. J. Eur. Ceram. Soc. 17 (1997) 407-413.

17. W Hong, P Hu, D Zhang, et al. Fabrication of ZrB_2-SiC ceramic composites by optimized gel-casting method. Ceram. Int. 2018, 44 (2018) 6037-6043.
18. L G Ma, Y Huang, J L Yang, et al. Control of the inner stresses in ceramic green bodies formed by gelcasting. Ceram. Int. 2006, 32 (2006) 93-98.
19. R He, P Hu, X Zhang, et al. Gelcasting of complex-shaped ZrB_2-SiC ultra high temperature ceramic components. Mater. Sci. Eng. B. 556 (2012) 494-499.
20. S W Jiang, T Matsukawa, S Tanaka, et al. Effects of powder characteristics, solid loading and dispersant on bubble content in aqueous alumina slurries. J. Eur. Ceram. Soc. 27 (2007) 879-885.
21. S Maleksaeedi, M H Paydar, J Ma. Centrifugal gel casting: a combined process for the consolidation of homogenous and reliable ceramics. J. Am. Ceram. Soc. 93 (2010) 413-419.
22. A Harabi, F Bouzerara, S Condom. Preparation and characterization of tubular membrane supports using centrifugal casting. Desalin. Water Treat. 6 (2009) 222-226.
23. J C Chang, B V Velamakanni, F F Lange, et al. Centrifugal consolidation of Al_2O_3 and Al_2O_3/ZrO_2 composite slurries vs interparticle potentials: particle packing and mass segregation. J. Am. Ceram. Soc. 74 (2005) 2201-2204.
24. W Huisman, T Graule, L J Gauckler. Alumina of high reliability by centrifugal casting. J. Eur. Ceram. Soc. 15 (1995) 811-821.
25. J A Lewis. Colloidal processing of ceramics. J. Am. Ceram. Soc. 83 (2000) 2341-2359.

Figures

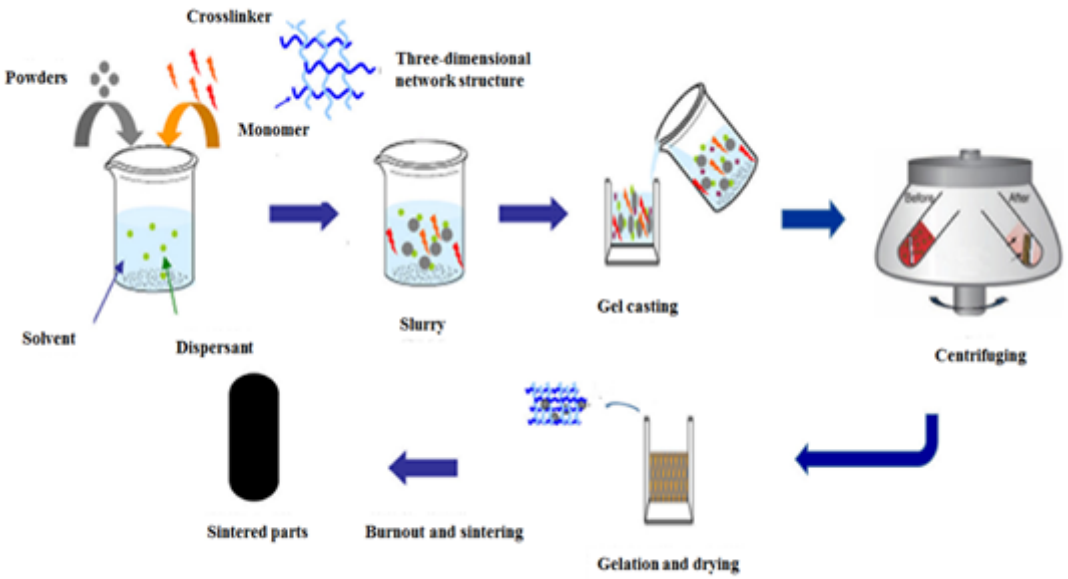

Figure 1

The flow chart of the centrifugal gel-casting process.

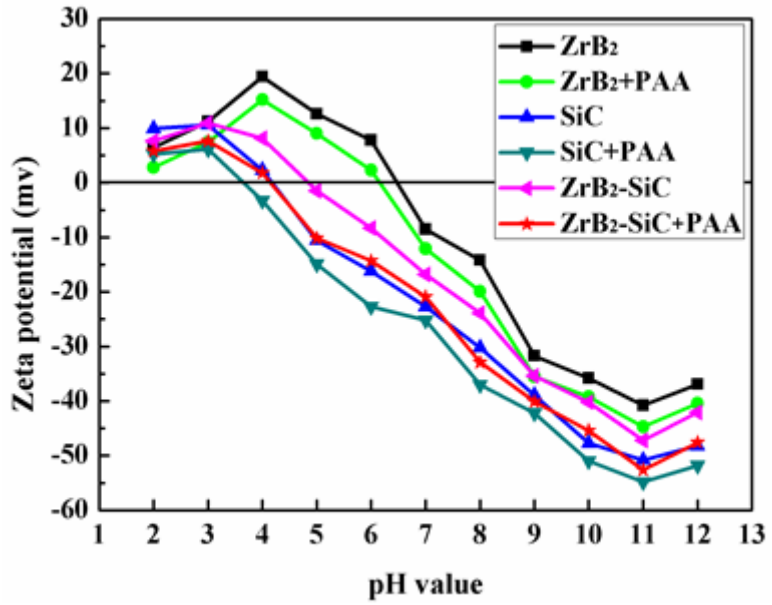

Figure 4

The Zeta potential as a function of pH for ZrB2-SiC suspensions with 0.5 wt.% and without PAA dispersant

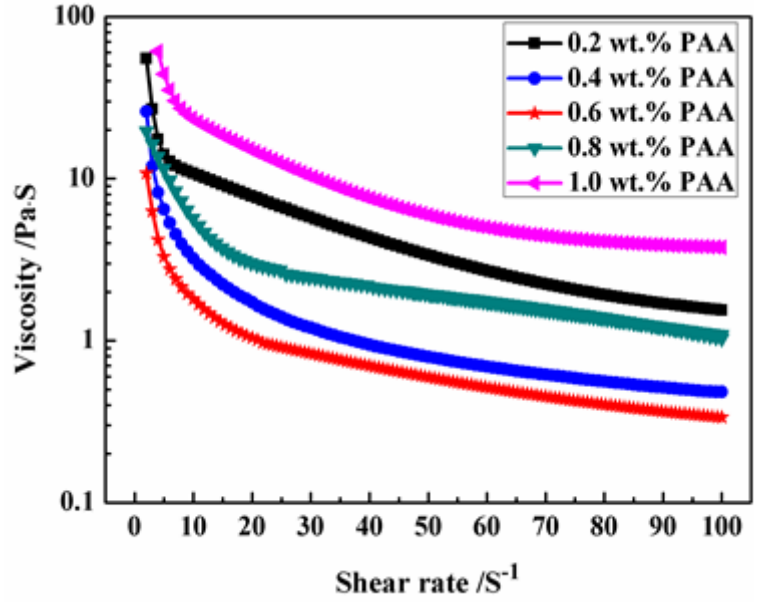

Figure 6

The effect of dispersant concentration on the viscosity of ZrB2-SiC suspension (30 vol.% solid loading at pH 11)

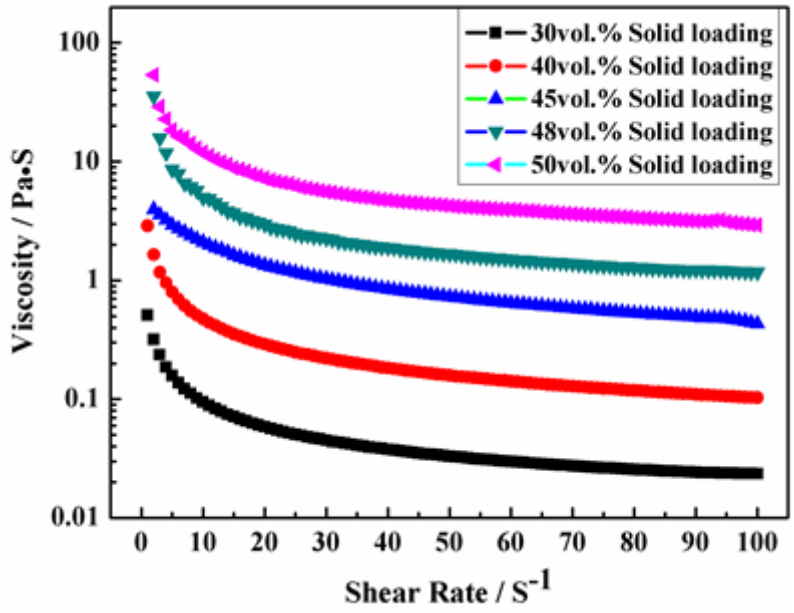

Figure 8

Effect of solid loading on the viscosity of ZrB2-SiC suspensions (0.6 wt.% PAA dispersant at pH 11)

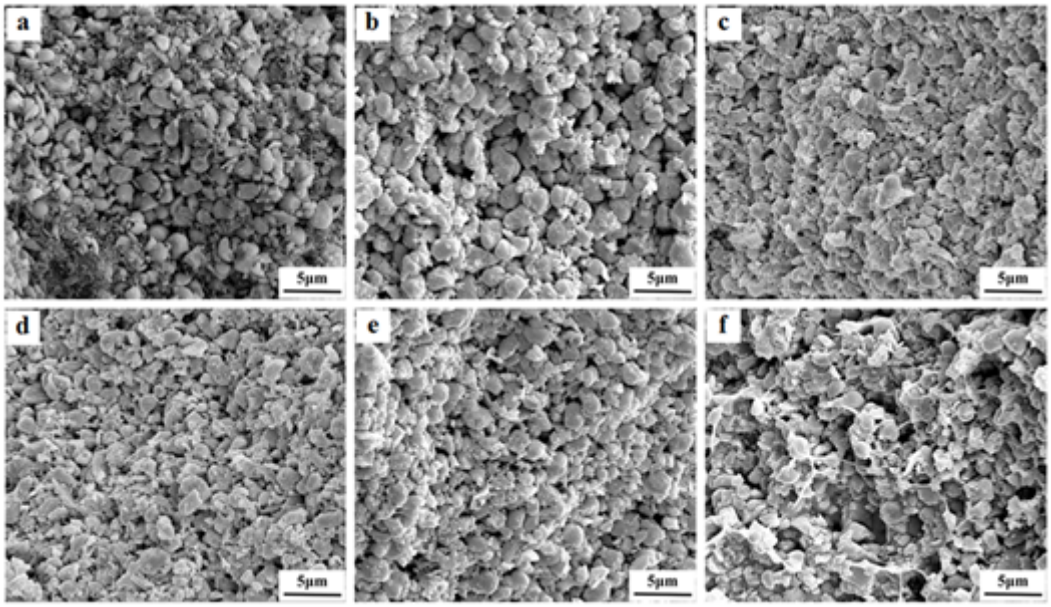

Figure 9

The effect of monomer content on the microstructure of green ZrB2-SiC ceramics. a. 2wt.%; b. 3wt.%; c. 3.5wt.%; d. 4wt.%; e. 4.5wt.%; f. 5wt.%

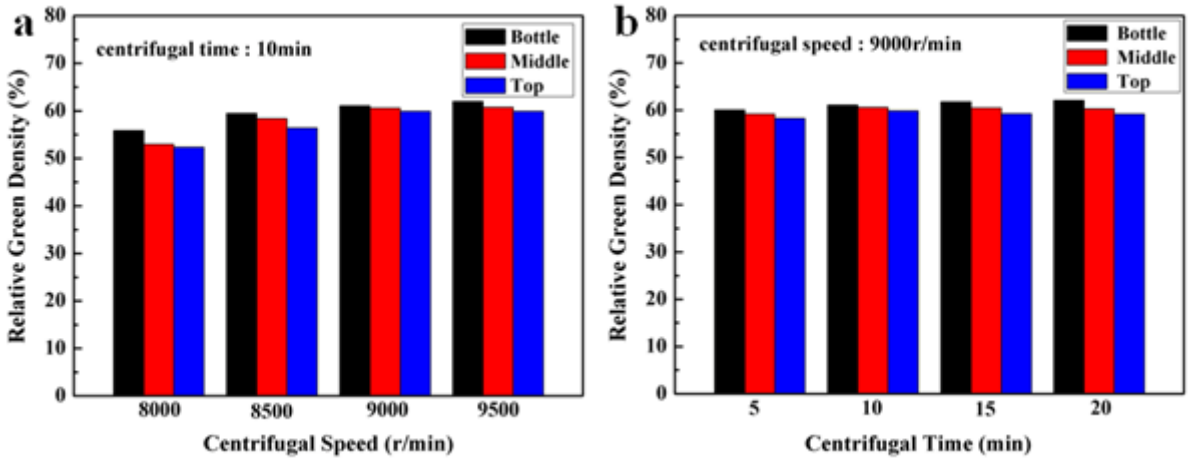

Figure 11

The relative green density of ZrB2-SiC ceramics with different centrifugal speed (a) and centrifugal time (b)

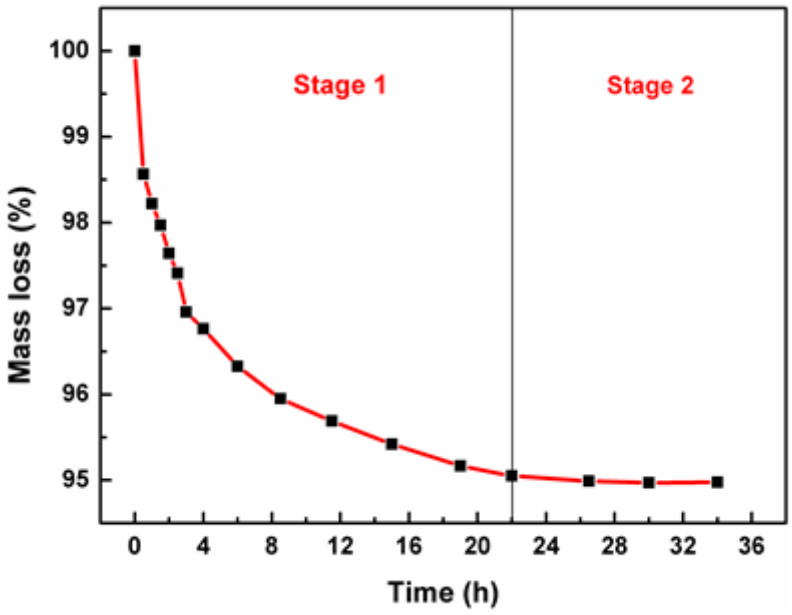

Figure 13

The mass loss of the ZrB2-SiC green bodies as a function of drying time.

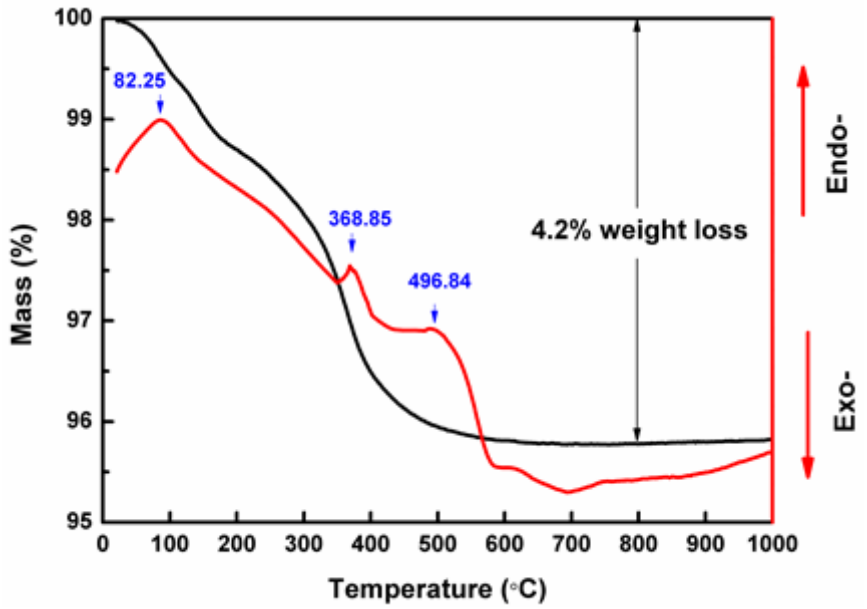

Figure 15

The TG-DSC curve of the ZrB2-SiC green bodies

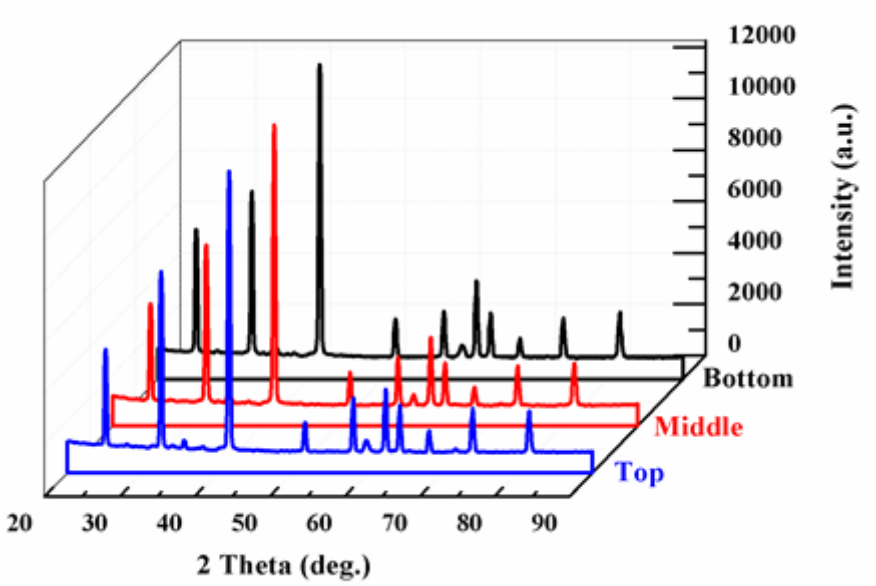

Figure 17

The XRD patterns of sintered ZrB2-SiC ceramics from the bottom to the top

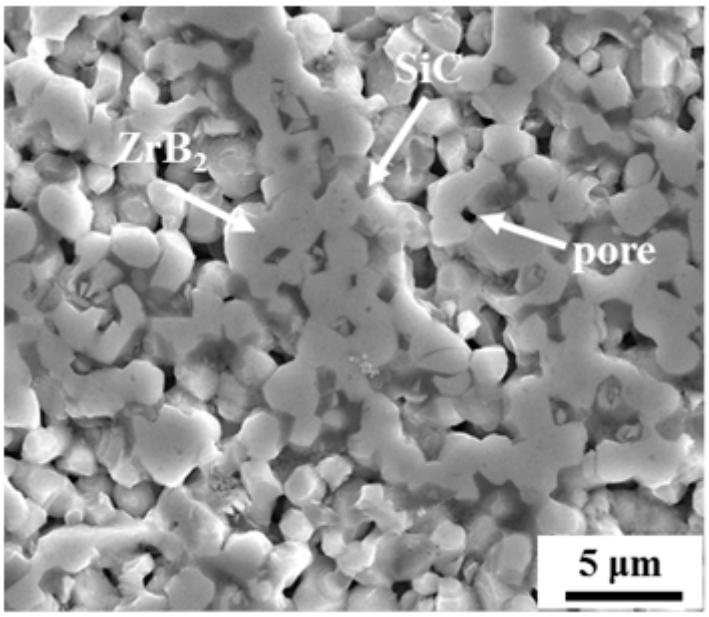

Figure 19

the microstructure of the polished surface of sintered ZrB2-SiC ceramics at 2000°C for 1h.